

Normal-state transport properties of $\text{Bi}_{2+x}\text{Sr}_{2-y}\text{CuO}_{6\pm\delta}$ crystals

S. Martin, A. T. Fiory, R. M. Fleming, L. F. Schneemeyer, and J. V. Waszczak
AT&T Bell Laboratories, Murray Hill, New Jersey 07974

(Received 19 September 1989)

Transport anisotropies of $\rho_c/\rho_{ab} \approx 10^4$ to 10^5 were measured for superconducting and nonsuperconducting $\text{Bi}_{2+x}\text{Sr}_{2-y}\text{CuO}_{6\pm\delta}$ crystals. In superconducting samples ρ_{ab} increases linearly with temperature from just above $T_c \approx 7$ to 700 K. The implication of the ρ_{ab} results is that classical electron-phonon scattering mechanisms are inadequate. The anisotropy and T_c for various layered superconductor systems are compared. In all crystals studied ρ_c is nonmetallic, varying as a power law $T^{-\alpha}$, $\alpha \approx 0.5-1$.

A characteristic feature of the high- T_c layered superconductors is the extreme two dimensionality of their physical properties. Transport anisotropy studies are hence very significant for establishing the role of the coupling between Cu-O planes on the mechanism of high- T_c superconductivity. Previous measurements in Y-Ba-Cu-O crystals suggested resistivity anisotropies of $\approx 10^2$ for samples with $T_c = 90$ K,^{1,2} and $\approx 10^3$ for 60-K samples.² In Bi-Sr-Ca-Cu-O crystals even larger anisotropies of $\approx 10^3$ to 10^5 were measured,^{3,4} giving rise to two-dimensional (2D) phase fluctuations near the superconducting transition.³ Similar behavior was recently reported for Tl-Ba-Ca-Cu-O thin films.⁵ Presently, the mechanism of charge transport perpendicular to the Cu-O planes is far from being clearly established, owing to the range of anisotropy values and the different types of temperature dependences reported by various groups.^{1-3,6-8} The reasons for the lack of a consensus include experimental uncertainties such as nonuniform composition, defect mediated hopping of carriers, inhomogeneous current flow, contributions from ρ_{ab} , improper deconvolution of anisotropic current flow, and contact misalignment. A further issue in understanding high- T_c superconductivity concerns the applicability of conventional electron-phonon scattering mechanisms to the description of normal-state transport properties. However, the problem can be addressed clearly only by normal-state measurements at temperatures well below the typical high T_c 's of 80-90 K. In this respect studies of the transport properties in the low- T_c , single-layer Bi-Sr-Cu-O compound are very promising for gaining insight into the behavior of the closely related high- T_c cuprates.

We report here transport anisotropy measurements on $\text{Bi}_{2+x}\text{Sr}_{2-y}\text{CuO}_{6\pm\delta}$ crystals which are superconducting with $T_c = 6.5-8.5$ K, or nonsuperconducting, depending upon the Sr/Bi ratio in the melt composition and the oxygen partial pressure (P_{O_2}) during growth.⁹ We find $\rho_c/\rho_{ab} = 5 \times 10^4$ to 2×10^5 at $T \approx T_c$ for both types of samples. The superconducting crystals show a strikingly linear temperature dependence of $\rho_{ab}(T)$ from just above T_c to 700 K, suggesting an extraordinarily small value of the transport Debye temperature of $\Theta_D^* \approx 35$ K in the context of a classical Bloch-Grüneisen (BG) treatment of electron-phonon scattering. In nonsuperconducting crystals $\rho_{ab}(T)$ shows a logarithmic upturn below T_{min}

$= 20-70$ K and a linearity above T_{min} . The resistivity perpendicular to the Cu-O planes is found to be of the nonmetallic form $\rho_c \propto T^{-\alpha}$ with $\alpha \approx 0.5-1$. Also presented are transport anisotropies in several dichalcogenides and in $\text{YBa}_2\text{Cu}_3\text{O}_{7-\delta}$ crystals where we find $\rho_c/\rho_{ab} \approx 10^3$ for $T_c \approx 60$ K and $\approx 10^2$ for $T_c \approx 90$ K.

Crystals of $\text{Bi}_{2+x}\text{Sr}_{2-y}\text{CuO}_{6\pm\delta}$ ("2:2:0:1") were grown in an alkali-halide flux and crystals of $\text{YBa}_2\text{Cu}_3\text{O}_{7-\delta}$ ("1:2:3") in a BaCuO_2 -CuO flux, as described previously.⁹ The notations 2:2:0:1 and 1:2:3 are used herein generally, rather than for specific compositions. We should emphasize that studies on 2:2:0:1 ceramic samples are revealing a complex phase diagram, implying that the structure of a crystal grown under specific conditions cannot be easily asserted.¹⁰ Typical crystals are platelets 1 mm across and $4 \mu\text{m}$ (2:2:0:1) or $50 \mu\text{m}$ (1:2:3) thick. High-quality contacts of low resistance were made by using an Ag paste which was cured in O_2 at 250°C . The resistivity components were measured using a generalization of the Montgomery method with the contacts placed on the ab -plane surfaces.³

Figure 1(a) shows the temperature dependence of the in-plane resistivity ρ_{ab} for two 2:2:0:1 crystals grown under conditions indicated. In the nonsuperconducting sample ρ_{ab} has a minimum at $T_{\text{min}} = 70$ K, with a slope of $\Delta\rho_{ab}/\Delta T = 1.88 \mu\Omega \text{ cm/K}$ above T_{min} . The extrapolated residual resistivity of $\rho_0 = 800 \mu\Omega \text{ cm}$ can be used to estimate a disorder parameter of $(k_{\text{Fl}})_{ab} = 3.7$. We found that by increasing the Sr/Bi melt ratio T_{min} decreases. By choosing a reduced P_{O_2} of 4% (of 1 atm) during growth, we obtained superconducting crystals with $T_c = 6.5-8.5$ K. In Fig. 1(a) the superconducting sample shows a remarkable linearity of ρ_{ab} from above T_c to 700 K. The $\rho_{ab} = 0$ transition is at $T_c = 6.5$ K. We obtain a slope of $\Delta\rho_{ab}/\Delta T = 0.74 \mu\Omega \text{ cm/K}$ and a residual resistivity of $\rho_0 = 70 \mu\Omega \text{ cm}$, which yields $(k_{\text{Fl}})_{ab} = 43$. For a superconducting sample with $T_c = 8.5$ K the corresponding values are $\Delta\rho_{ab}/\Delta T = 1.06 \mu\Omega \text{ cm/K}$, $\rho_0 = 100 \mu\Omega \text{ cm}$ and $(k_{\text{Fl}})_{ab} = 30$. In both cases the values of the disorder parameter indicate clean-limit superconductivity. Xiao *et al.*¹¹ reported measurements on ceramic samples of 2:2:0:1, where a linear temperature-dependent resistivity was observed from 10 to 300 K with $T_c = 7$ K; however, the data reflect a polycrystalline average of ρ_{ab} and ρ_c .

The linear temperature dependence of the in-plane

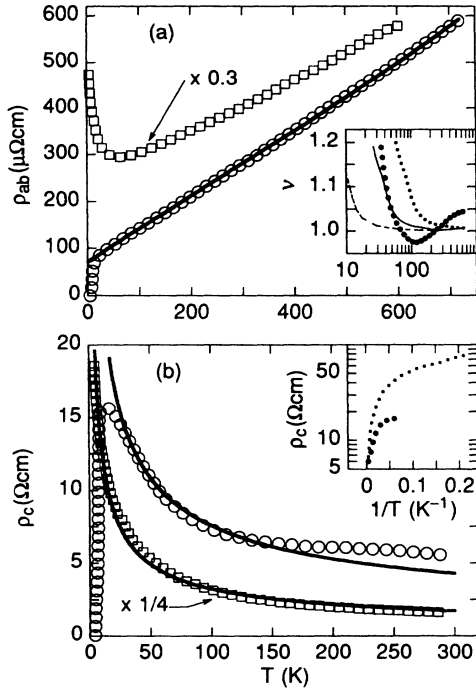


FIG. 1. In-plane (a) and out-of-plane (b) resistivities measured in 2:2:0:1 crystals: a nonsuperconductor (\square) grown with $\text{Sr/Bi}=1.22$ and $P_{\text{O}_2}=20\%$, and a superconductor (\circ), with $\text{Sr/Bi}=1.0$ and $P_{\text{O}_2}=4\%$. Curve in (a) is a fit assuming BG; curves in (b) are power-law fits. Inset (a) shows $\nu = d[\ln(\rho_{ab} - \rho_0)]/d[\ln T]$ vs T for the superconducting sample (\bullet) as compared with BG fits with $\Theta_D^* = 10$ K (dashed), 35 K (solid), and 80 K (dotted). Inset (b) illustrates ρ_c is non-Arrhenius.

resistivity is one of the characteristic features of normal-state transport in high- T_c superconductors. Novel models of the mechanism of high- T_c superconductivity predicting $\rho_{ab} \propto T$ include the resonating-valence-bond (RVB) model by Anderson and Zhou,¹² the quantum percolation model by Phillips,¹³ and the marginal Fermi-liquid model by Varma *et al.*¹⁴ Until recently, measurements of the normal-state properties in high- T_c materials have not provided especially strong support for novel types of charge transport. It was possible to argue that classical electron-phonon scattering as described by the BG model is valid if $T_c \approx 90$ K.¹⁵ The BG model predicts in 3D an initial T^5 increase of the resistivity for $T < \Theta_D^*$ and a linear temperature dependence for $T > \Theta_D^*$, where the transport Debye temperature Θ_D^* can be typically a factor of 2–4 smaller than the thermodynamic Debye temperature Θ_D for materials with a small k_F . For 1:2:3 Θ_D^* was found to be as low as ≈ 200 K.¹⁵ Thus down to $T_c \approx 90$ K the deviation would not be substantial enough to be apparent.

The low temperature behavior of ρ_{ab} shown in Fig. 1(a) for the nonsuperconducting sample is found to be caused by weak localization effects in 2D which are studied in detail elsewhere.¹⁶ For the superconducting sample a BG fit with $\Theta_D^* = 35$ K is shown as the nearly linear solid line. In the inset of Fig. 1(a) the logarithmic derivative $\nu = d[\ln(\rho_{ab} - \rho_0)]/d[\ln T]$ is plotted versus T . The sensitivity of ν to the choice of Θ_D^* is analyzed in detail by plot-

ting the data (denoted by \bullet) and, for comparison, BG fits with $\Theta_D^* = 10$ K (dashed curve), 35 K (solid curve), and 80 K (dotted curve). The data show a smooth decrease from $\nu = 1.05$ at 700 K to 0.97 at 120 K followed by a pronounced increase at lower temperatures. Within a deviation of $\pm 5\%$ the linearity of ρ_{ab} with T can be asserted over a range of $T = 50$ –700 K. A characteristic test of BG behavior is the onset of the nonlinearity $\nu > 1$ at low temperatures. The BG fit for $\Theta_D^* = 35$ K describes the data best, e.g., $\nu = 1.1$ is attained at $T = 40$ K in both the data and the fit. In contrast, neither $\Theta_D^* = 10$ K nor $\Theta_D^* = 80$ K adequately fit at the onset of nonlinearity. Although it is in best agreement with data, there is no clear understanding for such a small value of $\Theta_D^* = 35$ in terms of electron-phonon scattering. The thermodynamic Debye temperature is expected to be $\Theta_D \approx 350$ K, as found in the related high- T_c compound $\text{Bi}_2\text{Sr}_2\text{CaCuO}_8$ (2:2:1:2).¹⁷ A reasonable lower limit would therefore be $\Theta_D^* \approx 80$ K, which deviates from the data significantly. Interestingly, in the nonsuperconducting La-Sr and La-Ba cuprates the resistivities reported for polycrystalline materials resemble classical metals, deviating from linearity near 175–300 K.¹⁸

The lack of any saturation of $\rho_{ab}(T)$ up to 700 K is another similarity between 2:2:0:1 and the high- T_c materials. It implies a weak scattering mechanism and imposes an upper limit of $\lambda < 0.1$ for the electron-phonon coupling constant.¹⁹ If we assume only phonon scattering, then the resistivity slope provides the following quantitative estimate:¹⁹

$$\lambda = (0.246 \text{ eV}^{-2} \mu \Omega^{-1} \text{ cm}^{-1} / \text{K}) (\Delta \rho_{ab} / \Delta T) E_p^2,$$

where

$$E_p = (1.8 \times 10^3 \text{ eV \AA}) (1 + \lambda)^{1/2} / \lambda_L(0)$$

is the plasma energy and $\lambda_L(0)$ the London penetration depth. Taking $\lambda_L(0) = 3100$ \AA (Ref. 20) and an average slope of $0.9 \mu \Omega \text{ cm/K}$, we obtain $\lambda = 0.08$, suggesting particularly weak electron-phonon coupling.

Figure 1(b) shows the temperature dependence of the resistivity perpendicular to the Cu-O planes measured in the same 2:2:0:1 crystals. We find that ρ_c is nonmetallic and typically several orders of magnitude larger than ρ_{ab} , as in other layered cuprates.³ The nonmetallic behavior and the explicit form of the temperature dependence of ρ_c is an important issue for understanding the normal-state transport mechanism. In high- T_c materials the accessible low-temperature range is limited, thus obscuring the distinction between thermal activation and power-law behavior. In 2:2:0:1, however, measurements down to 4–8 K clearly indicate inconsistency with an Arrhenius law, as shown by the inset of Fig. 1(b), for both superconducting (denoted by \circ) and nonsuperconducting (denoted by \square) samples. Rather, better fits are obtained for a power law, $\rho_c \propto T^{-\alpha}$ with $\alpha = 0.61$ for the nonsuperconductor and 0.52 for the superconductor, as shown by the solid curves in Fig. 1(b). For comparison, we have previously found that $\alpha \approx 1$ adequately describes the temperature dependence of ρ_c in 2:2:1:2.²¹ In the RVB model of high- T_c superconductivity proposed by Anderson and Zhou,¹² the temperature dependence of ρ_c is expected to be inverse to

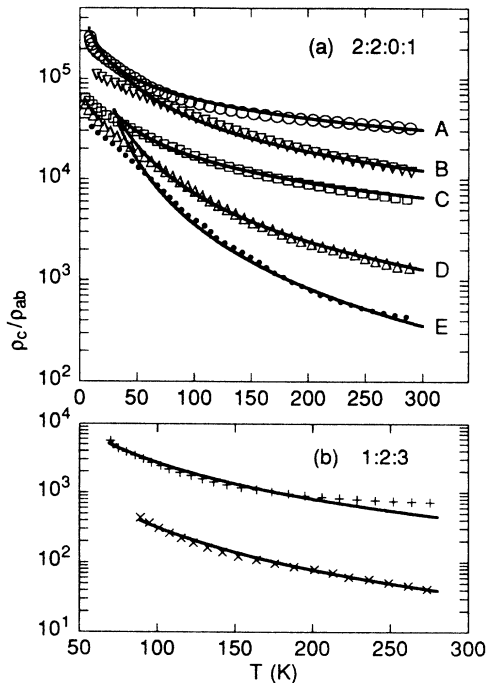


FIG. 2. Temperature dependence of resistivity anisotropies for crystals of (a) 2:2:0:1 and (b) 1:2:3 with $T_c = 90$ K (\times) and 60 K ($+$), grown under different conditions. Curves are power-law fits.

that of ρ_{ab} . Although it was observed in the high- T_c materials,^{1-3,21} our measurements in superconducting 2:2:0:1 crystals suggest a weaker power law for ρ_c than given simply by ρ_{ab}^{-1} .

Figure 2(a) shows the anisotropy ρ_c/ρ_{ab} for 2:2:0:1 samples grown with different Sr/Bi ratios in the melt composition and under different P_{O_2} . Sample *A* is the open circles and sample *C* is the open squares of Fig. 1. Samples *A* and *E* are superconducting with $T_c = 6.5$ and 8.5 K, respectively. For both samples $P_{O_2} = 4\%$, but Sr/Bi = 1 for *A* and 1.5 for *E*. The results imply that the change in Sr/Bi ratio in the melt has led to a decrease of the anisotropy by nearly an order of magnitude at T_c and two orders of magnitude at 300 K. The nonsuperconducting samples were grown under the following conditions: Sr/Bi = 1 (*B*), 1.22 (*C, D*) and $P_{O_2} = 20\%$ (*B, C*), 10% (*D*). The results in Fig. 2(a) suggest that the anisotropy becomes smaller as the Sr/Bi ratio is increased and P_{O_2} is decreased. The presence or absence of superconductivity, however, appears to be more strongly affected by P_{O_2} . The solid curves are fits to a power law $\rho_c/\rho_{ab} \propto T^{-\beta}$ with $\beta = 0.64$ (*A*), 1.07 (*B*), 0.84 (*C*), 1.57 (*D*), and 2.1 (*E*). Subtracting the residual resistivity $\rho_0 = 70 \mu\Omega \text{ cm}$, we obtain $\beta = 1.40$ for sample *A*. The results suggest that β tends to increase towards the value 2, as the anisotropy decreases. It is striking that the sample with the highest T_c , *E*, has a power-law exponent like that observed in high- T_c materials and predicted by the RVB model.

In Fig. 2(b) the resistivity anisotropies are plotted for Y-Ba-Cu-O crystals with $T_c \approx 90$ K (denoted by \times) and $T_c \approx 60$ K (denoted by $+$), where oxygen content was

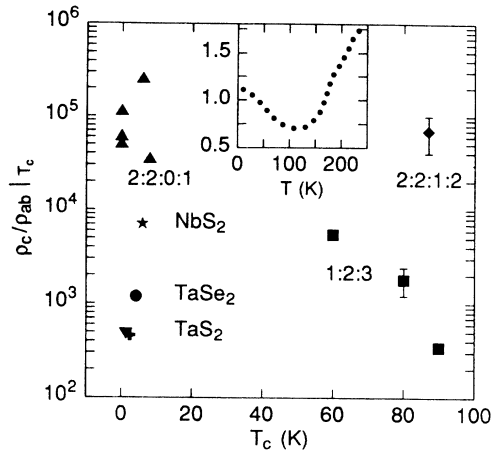


FIG. 3. Anisotropies just above T_c vs T_c for several layered cuprates and layered dichalcogenides (Refs. 22-24). The inset shows the temperature dependence for 2H-TaSe₂.

controlled by postannealing. We find that the lower- T_c crystal has an order of magnitude larger anisotropy, as also reported by Brawner, Wang, and Ong.² The temperature dependence of the anisotropy can be fit to a power law (solid lines) with $\beta = 1.73$ for the 60-K sample and 2.01 for the 90-K sample. Note again the tendency of β to approach the value 2 as the anisotropy decreases.

Furthermore, we find an indication of a higher T_c being correlated with a stronger coupling between the Cu-O planes. This feature is illustrated in Fig. 3, where the anisotropy values just above T_c are plotted versus T_c for the layered cuprates 2:2:0:1 ($T_c \approx 0, 6,$ and 8 K), 2:2:1:2 ($T_c \approx 87$ K), and 1:2:3 ($T_c \approx 60, 80,$ and 90 K). The 80-K 1:2:3 sample was annealed in an oxygen deficient atmosphere. The error bars shown for these data and for 2:2:1:2 indicate typical variations of the anisotropy measured in several samples. For comparison, results on layered dichalcogenides are also plotted. The temperature dependence of ρ_c/ρ_{ab} for 2H-TaSe₂ is drawn in the inset. This material undergoes a charge-density-wave transition at $T = 110$ K, below which we find that the anisotropy also increases with decreasing temperature, as in the layered cuprates. The remaining data are taken from other reports for 4Hb-TaS₂,²² 1T-TaS₂,²³ and 2H-NbS₂.²⁴ We see in Fig. 3 that the anisotropies in layered dichalcogenides are of similar magnitudes as in 1:2:3 samples ($\approx 10^2$ to 10^4). The layered Bi compounds are, however, more strongly anisotropic ($\approx 10^4$ to 10^5), the 2:2:0:1 samples showing variation with growth conditions.

In conclusion, a linear temperature dependence of the *ab*-plane resistivity from above $T_c \approx 7$ to 700 K was measured in superconducting 2:2:0:1 crystals, which cannot be accounted for by classical electron-phonon scattering. Nonmetallic behavior was found for transport perpendicular to the Cu-O planes, which appears to be universal. Anisotropies of $\rho_c/\rho_{ab} \approx 10^4$ to 10^5 were found near T_c and show tendencies to decrease with higher T_c .

We acknowledge many useful discussions with M. Gurvitch, P. B. Littlewood, J. C. Phillips, S. A. Sunshine, and C. M. Varma.

- ¹S. W. Tozer *et al.*, Phys. Rev. Lett. **59**, 1768 (1987).
²S. Hagen *et al.*, Phys. Rev. B **37**, 7928 (1988); D. A. Brawner, Z. Z. Wang, and N. P. Ong, Phys. Rev. B **40**, 9329 (1989).
³S. Martin *et al.*, Phys. Rev. Lett. **60**, 2194 (1988); *ibid.* **62**, 677 (1989).
⁴D. E. Farrell *et al.*, Phys. Rev. Lett. **63**, 782 (1989).
⁵D. H. Kim *et al.*, Phys. Rev. B **40**, 8834 (1989).
⁶Y. Iye *et al.*, Jpn. J. Appl. Phys. **26**, L1057 (1987); Physica C **153-155**, 26 (1988).
⁷L. I. Buranov *et al.*, Pis'ma Zh. Eksp. Teor. Fiz. **47**, 43 (1988) [JETP Lett. **47**, 51 (1988)].
⁸Y. Hidaka *et al.*, Rev. Electr. Commun. Lab. **36**, 567 (1988).
⁹L. F. Schneemeyer *et al.* (unpublished); Nature (London) **328**, 601 (1987).
¹⁰S. A. Sunshine *et al.* (unpublished).
¹¹G. Xiao *et al.*, Phys. Rev. B **38**, 11 824 (1988).
¹²P. W. Anderson and Z. Zhou, Phys. Rev. Lett. **60**, 132 (1988); *ibid.* **60**, 2257 (1988).
¹³J. C. Phillips, Phys. Rev. B **40**, 7348 (1989).
¹⁴C. M. Varma *et al.*, Phys. Rev. Lett. **63**, 1996 (1989).
¹⁵S. Martin *et al.*, Phys. Rev. B **39**, 9611 (1989).
¹⁶A. T. Fiory *et al.* (unpublished).
¹⁷J. E. Graebner (private communication).
¹⁸B. Raveau and C. Michel, in *Novel Superconductivity*, edited by S. A. Wolf and V. Z. Kresin (Plenum, New York, 1987), p. 599.
¹⁹M. Gurvitch and A. T. Fiory, Phys. Rev. Lett. **59**, 1337 (1987).
²⁰ $\lambda_L(0)$ was obtained from the 2300 Å value for La-Sr-Cu-O and scaling the copper density; D. R. Harshman (private communication).
²¹S. Martin *et al.*, Appl. Phys. Lett. **54**, 72 (1989).
²²W. J. Wattamaniuk, J. P. Tidman, and R. F. Frindt, Phys. Rev. Lett. **35**, 62 (1975).
²³P. D. Hamburger and F. J. Di Salvo, Physica B **99**, 173 (1980).
²⁴B. W. Pfalzgraf and H. Spreckels, J. Phys. C **27**, 4359 (1987).